EARTHQUAKE ENGINEERING AND STRUCTURAL DYNAMICS
*Earthquake Engng. Struct. Dyn.* **28**, 529–541 (1999)

# CONTROL LAW FOR VARIABLE DAMPING DEVICE DEFINED BY A NON-LINEAR DIFFERENTIAL EQUATION

KAZUHIKO YAMADA*,†
*Kobori Research Complex, Kajima Corporation, KI Building, 6-5-30 Akasaka, Minato-ku, Tokyo 107-8502, Japan*

## SUMMARY

This paper proposes a non-linear control law for a variable damping device (VDD) aimed at reducing structural seismic responses. The VDD is attached to the structure by an auxiliary spring element composing a non-linear Maxwell element. The VDD's damping coefficient is adjusted to control the reactive internal force in the non-linear Maxwell element. A large controlled force is thus produced with little external power required to adjust the VDD's damping coefficient. The proposed control law defines the rate or increment of the VDD's damping coefficient at a certain moment by a differential equation or its discretized form. The controlled force vs. deformation relation plots parallelogram-like hysteretic curves, which indicates quick action and energy dissipation. Fundamental characteristics of an SDOF model with the VDD controlled by the proposed law are examined for impulse, sin and seismic excitations. The law for the SDOF model is extended to one for an MDOF model. The control effect for a 3DOF model is examined by numerical experiments. Copyright © 1999 John Wiley & Sons, Ltd.

KEY WORDS: variable damping device; non-linear control; non-linear Maxwell element; non-linear differential equation; seismic response

## INTRODUCTION

To dissipate energy caused by an earthquake, many structures are provided with passive dampers.[1–6] When dampers are installed between storeys, they are accompanied by auxiliary spring elements (ASE) such as braces and walls. Unless the ASE's stiffness is large enough, its response delay dulls the damper's ability. The damper's stiffness must be considered even if it is large enough to span storey height by itself. We must necessarily examine the damper's effects as a Maxwell element. Next, for maximum damping effect, let us assume a high-capacity damper. In this case, the damper works like a rigid element. Thus, the damper force may exceed its allowance during a large earthquake. It can restrain structural deformation due to static loads, but it does not dissipate energy due to dynamic loads. Furthermore, a structure may be subjected to more earthquake energy because the high-capacity damper accompanying the ASE shortens the

*Correspondence to: Kazuhiko Yamada, Kobori Research Complex, Kajima Corporation, KI Building, 6-5-30 Akasaka, Minato-ku, Tokyo 107-8502, Japan. E-mail: kazu@krc.kajima.co.jp
† Senior Research Engineer

CCC 0098–8847/99/050529–13$17·50

*Received 31 May 1998*
*Revised 9 November 1998*

structure's natural frequency. The passive damper's effect depends on the ASE's stiffness and the earthquake's characteristics and strength levels as well as the damper's capacity.

A better way may be to change the damper's damping coefficient.[7–11] As a semi-active control system with little external power, a variable damping device (VDD) can control a reactive internal force in the range of the VDD's capacity, which follows a velocity feedback law as in an active control system. Recent research[12–16] indicates that the VDD is more active when comprised of a nonlinear Maxwell element with the ASE than by itself, and controlled by the law based on energy dissipation. The non-linear Maxwell element can, in fact, dissipate more energy than a linear damper, drawing a hysteretic controlled force vs. deformation relation. The non-linear Maxwell element restrains deformation with little delay like a spring when the VDD's damping coefficient is large, whereas it dissipates energy as a damper when the VDD's damping coefficient is not large. Thus, it can appropriately utilize the ability of either. A control law for the anticipated effect can be introduced, based on an optimization problem. However, it is usually complex. A control law should be simple for practical purposes.

The dynamics of a structure with the VDD is non-linear. Recent research[17,18] on non-linear dynamical systems shows that even a simple non-linear term makes the system behave complexly; and that we can examine dynamical behaviour in the neighbourhood of steady states, considering the non-linear term's influence expanded by the Taylor series. These facts can be utilized in design, i.e. we can add a simple non-linear term into a linear system, which makes the system serve our design purpose.

Therefore, in this paper, we add a simple non-linear term to the VDD's damping coefficient, and then introduce a control law. This law aims at dissipating as much energy as possible and restraining the controlled force. Simply, the non-linear term is assumed to be a function of the controlled force. Because the VDD's damping coefficient is related only to the controlled force, the control law can be easily applied to an MDOF model. The resulting controlled force vs. deformation relation draws parallelogram-like hysteretic curves. Thus, the expected effect of the non-linear Maxwell element is similar to that of yielding of structural elements.

The following first proposes a control law for a VDD attached to an SDOF model. Next, it examines the basic performance of the SDOF model with the VDD controlled by the proposed control law for impulse, sine and seismic excitations. Then, it extends to one for an MDOF model. The control effect is finally examined by numerical experiments on a 3DOF model.

## CONTROL LAW FOR THE SDOF MODEL

### *Structural dynamics*

Let us consider a single-degree-of-freedom (SDOF) structural model under a seismic excitation. As shown in Figure 1, this model consists of not only a structural mass and a spring element but also of a Variable Damping Device (VDD) and an Auxiliary Spring Element (ASE). The VDD whose damping coefficient can be adjusted is installed between the mass and the ASE so that the VDD and the ASE compose a non-linear Maxwell element. Adjusting the VDD's damping coefficient controls the reactive internal force in the non-linear Maxwell element. A large controlled force is thus produced in the non-linear Maxwell element, with only a little external energy required to adjust the VDD's damping coefficient.

 

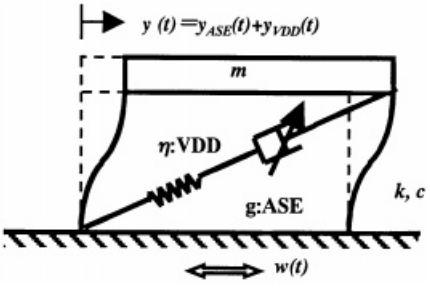


Figure 1. SDOF model with ASE and VDD

Then, structural dynamics at time $t$ for a seismic excitation is expressed by

$$my''(t) + cy'(t) + ky(t) + u(t) = -mw(t) \tag{1}$$

$$u'(t) = gy'(t) - \frac{g}{\eta(t)}u(t) \tag{2}$$

where $y''(t)$, $y'(t)$ and $y(t)$ represent the model's response acceleration, velocity and displacement, respectively; $m$, $c$ and $k$ are the structural mass, damping and stiffness, respectively; $u(t)$ and $u'(t)$ are the controlled force in the non-linear Maxwell element and its rate, respectively; $w(t)$ is the acceleration at the structural basement of the seismic excitation; $g$ is the ASE's stiffness; and $\eta(t)$ is the VDD's damping coefficient.

*VDD's damping coefficient*

Let us suppose that the VDD's damping coefficient is non-linearly related to the controlled force, and express it by a power series:

$$\eta(t) = \eta_0 + \lambda_1 u(t) + \tfrac{1}{2}\lambda_2 u(t)^2 + \tfrac{1}{3!}\lambda_3 u(t)^3 + \tfrac{1}{4!}\lambda_4 u(t)^4 + \cdots . \tag{3}$$

Thus, $\eta(t)$ implicitly depends on velocity and displacement through equations (1) and (2). In equation (3), if the odd-order terms is active, $\eta(t)$ in the positive direction of $u(t)$ differs from that in the negative direction. Thus, the odd-order terms should be inactive. The second-order term must be representative of the even-order terms so that the other even terms are not considered in this paper. Then, equation (2) becomes

$$u'(t) = gy'(t) - \frac{g}{\eta_0}u(t)\left(1 + \frac{\lambda_2}{2\eta_0}u(t)^2\right)^{-1} = gy'(t) - \frac{g}{\eta_0}u(t)\left(1 - \frac{\lambda_2}{2\eta_0}u(t)^2 + \cdots\right) \tag{4}$$

With positive $\lambda_2$, the larger the controlled force, the larger the damping coefficient. At that time, the larger the controlled force, the more accelerated the increment. However, with negative $\lambda_2$, the larger the controlled force, the smaller the increment. Then, the controlled force may possess a limit. Hence, aiming at restraining the controlled force, let us assume

$$\eta(t) = \eta_0 - \frac{\lambda}{2}u(t)^2 \tag{5}$$

 

where $\eta_0$ is the maximum damping coefficient of the VDD, and $\lambda = -\lambda_2 > 0$ is called a non-linear factor. The non-linear factor $\lambda$ is a given parameter that adjusts the non-linear influence on the damping coefficient vs. controlled force relationship. The larger the non-linear factor $\lambda$, the more sharply the VDD's damping coefficient $\eta$ decreases. We can understand the non-linear influence from the equation expanded by the Taylor series. As shown in equation (4), $u(t)^3$ and other high-order terms are small for small controlled force. Thus, the controlled force is almost equivalent to the force in a linear Maxwell element with stiffness $g$ and damping coefficient $\eta_0$. In particular, when $u(t)$ is very small, the controlled force becomes the force in a spring element with stiffness $g$. However, when the controlled force becomes large, high-order terms of $u(t)$ become so dominant in equation (4) that the rate, i.e. the increment per unit time, of the controlled force is restrained. When the increment can be regarded as approximately zero, i.e. $u'(t) \approx 0$, then $u(t) \approx \eta(t)y'(t)$. The controlled force then works like the force provided by a non-linear damper.

The slope of the controlled force vs. deformation ($u$–$y$) relation is steep for small deformation but flat for large deformation, so the $u$–$y$ relation draws parallelogram-like hysteretic curves. The area surrounded by the closed hysteretic curve indicates the energy dissipation.

*Stability condition*

Let us introduce a stability condition, based on energy balance. Substitute equation (2) multiplied by $u(t)$ into equation (1) multiplied by $y'(t)$ and integrate the resulting equation from $t_1$ to $t_2$. Then

$$[\tfrac{1}{2}my'(t_2)^2 + \tfrac{1}{2}ky(t_2)^2 - \tfrac{1}{2}my'(t_1)^2 - \tfrac{1}{2}ky(t_1)^2] + \left[\int_{t_1}^{t_2} cy'(t)^2 \mathrm{d}t\right] + \left[\frac{1}{2g}\{u(t_2)^2 - u(t_1)^2\} + \int_{t_1}^{t_2} \frac{1}{\eta(t)}u(t)^2\,\mathrm{d}t\right] = \left[-\int_{t_1}^{t_2} my'(t)w(t)\,\mathrm{d}t\right] \tag{6}$$

The four terms inside the brackets are called the vibration, damping, controlled force and input energies, respectively. The term $\int_{t_1}^{t_2}(1/\eta(t))u(t)^2\,\mathrm{d}t$ indicates the energy dissipation by the VDD between $t_1$ and $t_2$. To keep the energy dissipation continuous, $\eta(t)$ must be positive. The term $(1/2g)\{u(t_2)^2 - u(t_1)^2\}$ represents the energy stored in the ASE. On condition that the initial state at $t_1$ is still and that the end state at $t_2$ converges to still, the vibration energy and $(1/2g)\{u(t_2)^2 - u(t_1)^2\}$ should be zero. The structural damping and the VDD must dissipate the input energy during an earthquake. Therefore, the control law is stable as far as $\eta(t) > 0$ is kept under the assumed parameters.

*Control law*

A practical control law for the VDD is introduced by differentiating equation (5):

$$\eta'(t) = -\lambda u(t)u'(t) = -\lambda g y'_{\mathrm{ASE}}(t)u(t) = -\lambda g(y'(t) - u(t)/\eta(t))u(t), \tag{7}$$

where $y'_{\mathrm{ASE}} = (y'(t) - u(t)/\eta(t))$, which indicates the deformation rate in the ASE. A more practical control law is introduced by discretizing equation (7), considering control delay $\theta$:

$$\eta(t) = \eta(t-\theta) - \theta\lambda g y'_{\mathrm{ASE}}(t-\theta)u(t-\theta). \tag{8}$$

 

These control laws define the rate and increment of $\eta(t)$, that is, they dictate how much $\eta(t)$ should be increased or decreased in the future. The $\eta(t)$ should increase when $y'_{ASE}(t)$ and $u(t)$ have the different directions; however, it should decrease when $y'_{ASE}(t)$ and $u(t)$ have the same directions. The ASE can store strain energy when $\eta(t)$ is large, while the energy stored in the ASE is released and dissipated by a large deformation when $\eta(t)$ is small.

## BASIC PERFORMANCE OF CONTROLLED SDOF MODEL

Let us examine the basic performance of the proposed control law, using an SDOF model with $m = 1{\cdot}0$, $c = 0{\cdot}04\pi$ and $k = 4\pi^2$. It is assumed that the natural frequency and the damping factor of the model are 1·0 and 0·01, respectively; that the time interval $\Delta t$ for numerical computation is 0·01, and that the control delay $\theta$ is 0·01. The assumed parameters are dimensionless, so their units are unspecified. The following first examines the responses to impulse, sine and seismic excitations. Next, the influence of the parameters on the control effect is examined for various excitation levels. To compute responses, equations (1) and (2) are converted to one first-order differential equation in an extended state space whose state vector consists of the response velocity, the displacement and the controlled force.

### *Responses to impulse*

Now, we obtain the impulse response of the SDOF model with the non-linear Maxwell element controlled by the proposed law. Assume that $g = 4\pi^2$, $\eta_0 = \pi^2$ and $\lambda = 1{\cdot}0$, and that the initial velocity of the impulse is 2·0. The computational case is called Case VDD, which is compared with the cases for the same structural model with linear Maxwell elements assuming $\lambda = 0{\cdot}0$. These cases with $\eta_0 = \pi^2$, 3·0 and 2·34 are called Cases LNR-max, LNR-eqv and LNR-min, respectively. The assumed $\eta_0$ for Cases LNR-max and LNR-min are the resulting maximum and minimum of $\eta(t)$ for Case VDD. With the assumed $\eta_0$, the resulting maximum controlled force for Case-LNR-eqv is almost equal to that for Case-VDD.

The resulting controlled force vs. the displacement ($u$–$y$) relations are shown in Figure 2. As shown in the outermost curve of the $u$–$y$ relation in Figure 2(a), the controlled force for Case VDD works like an elastic-spring force at first, but does not linearly increase. The controlled force for large deformations is restrained from becoming large, but it dissipates a large amount of the

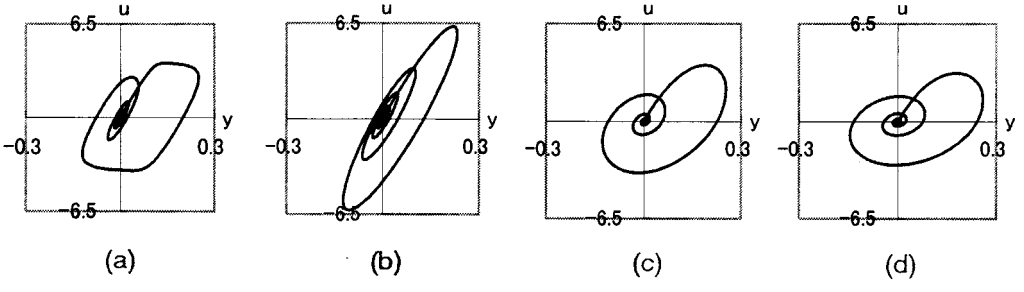


Figure 2. $u$–$y$ relations for impulse excitation: (a) VDD; (b) LNR-max; (c) LNR-eqv; (d) LNR-min

 

energy. For the later rounds when the deformation becomes small, the $u$–$y$ relation shows that the controlled force works like an elastic-spring force again. As a result, the $u$–$y$ relation draws parallelogram-like curves. The controlled force for Case LNR-max mostly works like an elastic-spring force with a damping, so the $u$-$y$ relation is elliptic. Although the large controlled force is required for Case-LNR-max, the response is slowly reduced. The controlled force for Case LNR-min more slowly makes action than that for Case-VDD so that the former is more slowly converges to zero displacement. The controlled force for Case-LNR-min is so small that the response is slowly reduced.

*Responses to sine excitation*

Let the above model be excited by sine waves $w(t) = w_0 sin(2\pi t)$ with $w_0 = 2{\cdot}0$ and $4{\cdot}0$, called S-2·0 and S-4·0, respectively. Figure 3 shows the resulting relations: (a) controlled force vs. displacement ($u$–$y$), (b) VDD's damping coefficient vs. controlled force ($\eta$–$u$), (c) VDD's damping coefficient vs. displacement ($\eta$–$y$) and (d) VDD's damping coefficient vs. velocity ($\eta$–$y'$).

For S-2·0, the $u$–$y$ relation is elliptic. That is, the controlled force works to reduce the responses just like the force in a Maxwell element. The $\eta$–$u$ relation lies on a parabolic curve, although the change in $\eta(t)$ is small. Despite the small change in $\eta(t)$, the $\eta$–$y$ and $\eta$–$y'$ relations plot butterfly-wing-like traces. The $\eta$–$y$ relation for the positive displacement moves counterclockwise, while the $\eta$–$y'$ relation for the positive velocity moves clockwise. This means that $\eta(t)$ cannot be defined by a one-to-one mapping of $y(t)$ or $y'(t)$.

For S-4·0, maximum velocity and displacement are more than twice those for S-2·0, being influenced by VDD's non-linearity. The $u$–$y$ relation plots parallelogram-like curves due to the change in $\eta(t)$ from 10·0 to 3·0. At some intervals during one cycle, $u(t)$ keeps certain positive/negative values, but changes linearly from positive to negative values or vice versa during

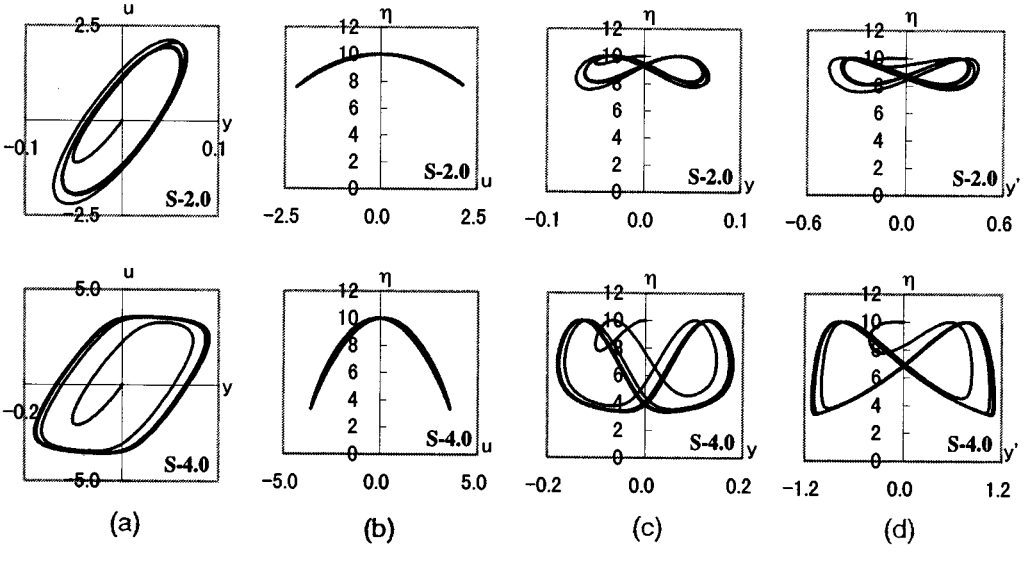


Figure 3. $u$–$y$, $\eta$–$u$, $\eta$–$y$ and $\eta$–$y'$ relations for S-2·0 and S-4·0: (a) $u - y$; (b) $\eta - u$; (c) $\eta - y$; (d) $\eta - y'$

 

other intervals. The $\eta$–$u$ relation plots a parabolic curve with a slight swell caused by the control delay. Due to the decrease in the VDD's damping coefficient, the $\eta$–$y$ and $\eta$–$y'$ relations plot butterfly-wing-like shapes with wider wings than those for S-2·0, keeping the direction of their trajectories. During the limit cycle, $y'(t)$ reaches its maximum value when $y(t)$ is near zero or *vice versa*. After $y(t)$ reaches zero, $\eta(t)$ marks its minimum and gradually increases later. On the other hand, when $y(t)$ is close to its maximum, $y'(t)$ changes its direction and $\eta(t)$ experiences a large increment to its maximum. Later, $\eta(t)$ quickly decreases when $y(t)$ returns to zero. The slope of the $u$–$y$ relation is steep when $\eta(t)$ is large, but is gradual when $\eta(t)$ is small.

*Responses to seismic excitations*

Next, the responses of the same model are computed for the seismic excitation of El Centro 1940 NS (El Centro). The maximum acceleration of El Centro is scaled to 2·0 and 8·0. The scaled excitations are called E-2·0 and E-8·0 after their maximum accelerations. The resulting $u$–$y$ and $\eta$–$y$ relations are shown in Figure 4.

$\eta(t)$ for E-2·0 changes so slightly that the controlled force works like the force in a Maxwell element and the $u$–$y$ relation plots an elliptic curve. $\eta(t)$ for E-8·0 changes from 10·0 to around 2·0. $\eta(t)$ has a large increment near when $y(t)$ experiences its extremums. Between the extremums of $y(t)$, $\eta(t)$ gradually decreases. As a result, the $u$–$y$ relation plots parallelogram-like curves.

*Parameter influence*

Let us examine how the parameters, ASE's stiffness $g$ and VDD's damping coefficient $\eta_0$ and non-linear factor $\lambda$ influence the responses for the different excitation levels. Let us assume the following trios:

$$(g, \eta_0, \lambda) = (4\pi^2, \pi^2, 1{\cdot}0), (8\pi^2, \pi^2, 1{\cdot}0), (\pi^2, \pi^2, 1{\cdot}0), (4\pi^2, \pi^2/2, 0{\cdot}5), (4\pi^2, 2\pi^2, 2{\cdot}0)$$

The responses of the assumed models are computed for various levels of the same sine waves and El Centro. However, the maximum accelerations of the sine waves are scaled to 0·2 to 2·0 with increments of 0·2 and those of El Centro are scaled to 0·5–4·0 with increments of 0·5. These excitations are called after their initial and maximum accelerations $w_{\max}$; for example, S-0·2 or E-4·0. The maximum response controlled force, the maximum response of the structural spring force and the minimum VDD's damping coefficient are called $u_{\max}$, $f_{\max}$ and $\eta_{\min}$, respectively.

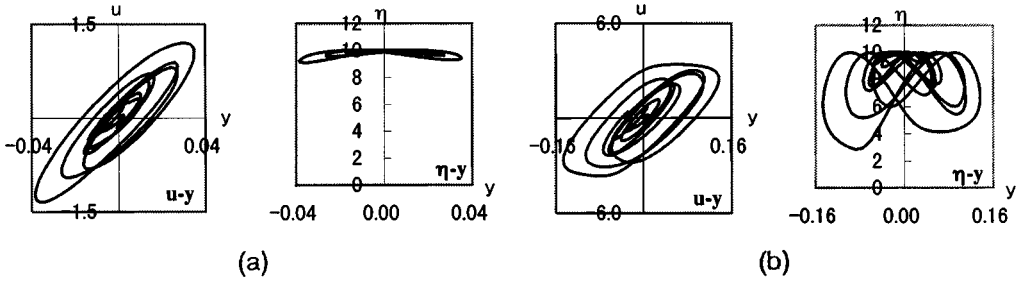


Figure 4. $u$–$y$ and $\eta$–$y$ relations for E-2·0 and E-8·0: (a) E-2.0; (b) E-8.0

 

Figure 5 shows the relations of $\eta_{max}$–$w_{max}$, $u_{max}$–$w_{max}$ and $f_{max}$–$w_{max}$ for each parameter trio. When $w_{max}$ is large, $\eta_{max}$ becomes small and the $u_{max}$–$w_{max}$ relation has a gradual slope. Because of the VDD's non-linearity, the responses for the large excitations are reduced less than those for the small excitations. Of the cases with the same $\eta_0$, the larger the $g$ cases, the smaller the responses. Since the ASE with large $g$ causes little phase delay, the controlled force for these cases can reduce the responses efficiently. Of the cases with the same $g$, the larger the $\eta_0$ case, the smaller the responses to the sine waves, as shown in Figure 5(a). This is because the large $\eta_0$ case has more ability to dissipate energy than the small $\eta_0$ case. However, the larger the $\eta_0$ case, the larger the responses to El Centro, as shown in Figure 5(b). This different tendency from that for the sine

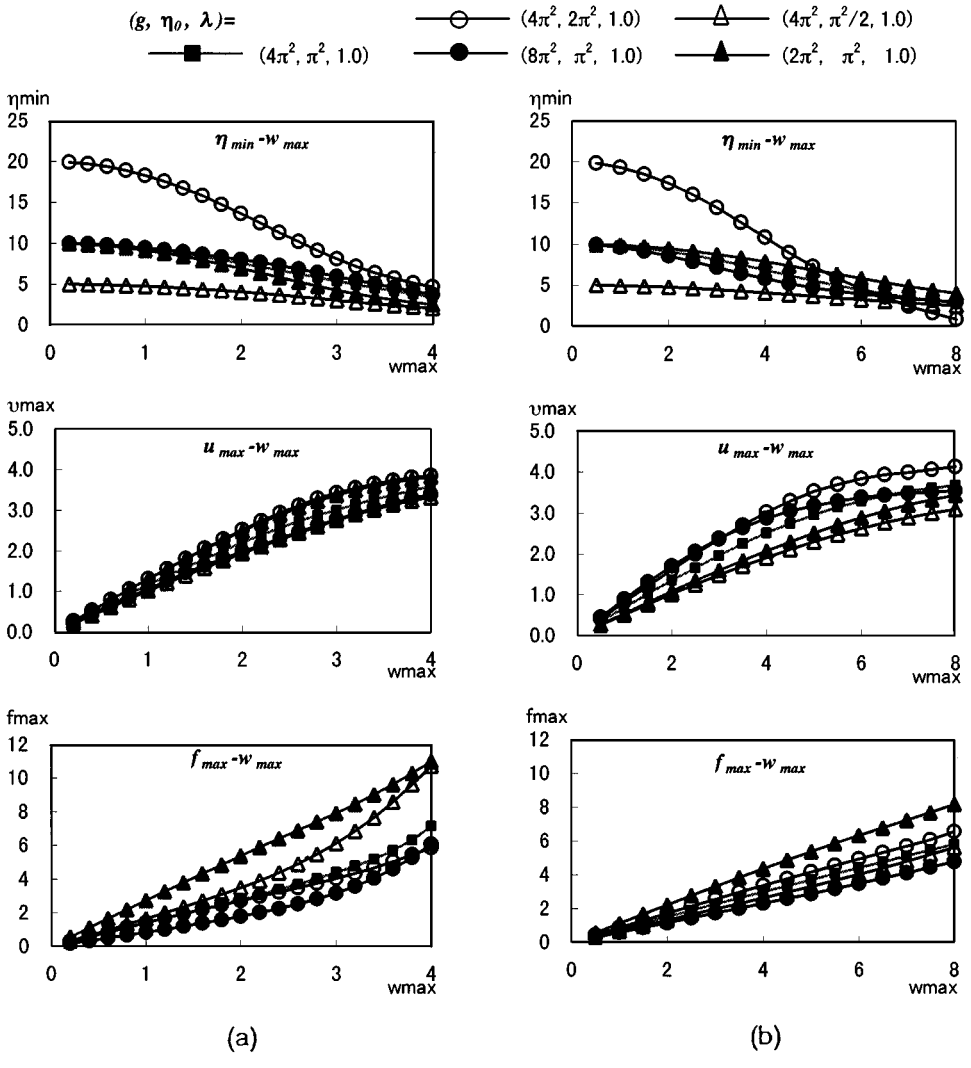


Figure 5. Relations of $u_{max}$, $f_{max}$ and $\eta_{min}$ vs. $w_{max}$ for sine waves and EL Centro: (a) sin wave; (b) El Centro

 

waves results from the dynamic characteristics of El Centro, which has larger power from 0·3 to 0·9 s than at 1·0 s. The natural period of the model with large $\eta_0/g$ is shortened by the influence of the non-linear Maxwell element, so that the model is subjected to more earthquake energy. Thus, the cases with large $\eta_0/g$ show larger responses to El Centro than those with small $\eta_0/g$. This suggests that the parameters in practice should be determined through simulation analyses for the assumed design excitation.

As described above, the basic performance of the SDOF model with the VDD controlled by the proposed law is examined for impulse, sine and seismic excitations.

## EXTENSION TO MDOF MODEL

### *MDOF structural model*

Next, let us extend the proposed control law to one for a multi-degree-of-freedom (MDOF) structural model with plural non-linear Maxwell elements comprising an ASE and a VDD. Assume that $n$-dimensional vectors $y''(t)$, $y'(t)$ and $y(t)$ represent the response acceleration, velocity and displacement, respectively, of an $n$DOF structural model at time $t$ relative to the structural basement; that $u(t)$ represents the $m$-dimensional controlled force vector by the $m$ pair of the non-linear Maxwell elements; and that $w(t)$ represents the excitation acceleration. The structural motion is expressed by

$$My''(t) + Cy'(t) + Ky(t) + Uu(t) = -MVw(t) \tag{9}$$

where $M$, $C$ and $K$ are the $n*n$-dimensional mass, damping and stiffness matrices, respectively, of the model; $V$ is the $n$-dimensional vector which indicates the DOF where the seismic excitation acts; and $U$ is the $n*m$-dimensional matrix which represents the DOF where the controlled forces act. When the controlled forces can act between DOF as shown in Figure 6, $U$ is expressed as

$$U = \begin{bmatrix} 1 & 0 & 0 \\ -1 & 1 & 0 \\ 0 & -1 & 1 \end{bmatrix} \tag{10}$$

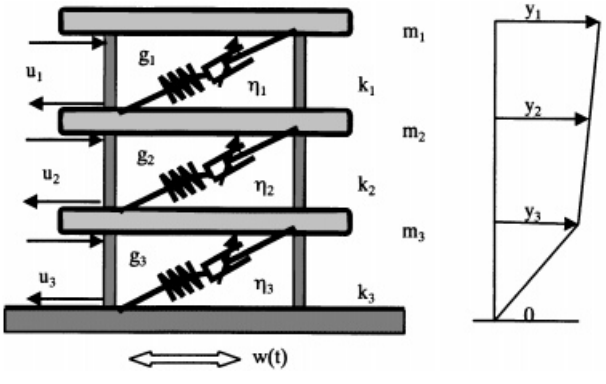


Figure 6. MDOF model with ASE and VDD

 

*Control law*

The control law expressed by equation (7) can be easily extended to one for the MDOF model. Considering the control delay $\theta$, let the $j$th VDD's damping coefficient $\eta_j(t)$ controlled by

$$\eta_j(t) = \eta_j(t-\theta) - \theta\lambda_j g_j y'_{\mathrm{ASE}_j}(t-\theta)u_j(t-\theta) \tag{11}$$

where $\lambda_j$, $g_j$, $y'_{\mathrm{ASE}j}(t)$ and $u_j(t)$ represent a non-linear factor for the $j$th VDD, the stiffness of the $j$th ASE, the deformation rate between the edges of the $j$th ASE, and the controlled force by the $j$th non-linear Maxwell element. The maximum $\eta_j(t)$ is assumed to be $\eta_{j0}$. By letting $U_j$ represent the $j$th column of $U$, the deformation and its rate between the DOF where the controlled force $u_j$ acts are expressed by $U_j^{\mathrm{T}}y(t)$and $U_j^{\mathrm{T}}y'(t)$, respectively. Thus, the control law can be expressed by the only information of the DOF which directly concerns the non-linear Maxwell element, that is

$$\eta_j(t) = \eta_j(t-\theta) - \theta\lambda_j g_j[U_j^{\mathrm{T}}y'(t-\theta) - u_j(t-\theta)/\eta_j(t-\theta)]u_j(t-\theta) \tag{12}$$

By letting $G = \mathrm{diag}\{g_j\}$ and $E(t) = \mathrm{diag}\{g_i/\eta_j(t)\}$, equation (2) is extended to

$$u'(t) = GU^{\mathrm{T}}y'(t) - E(t)u(t) \tag{13}$$

where diag$\{\ \}$ composes a diagonal matrix of a vector $\{\ \}$.

To compute the responses, equations (9) and (13) are combined, and then expressed by an extended state equation.

## APPLICATION TO 3DOF STRUCTURE

Let us examine the performance of the extended control law by numerical analyses applied to a three-storey structure. The structure is fitted with the three non-linear Maxwell elements comprising the ASE and the VDD between each storey. Let us model it as a 3DOF system, assuming the lumped masses at each floor and structural springs between storeys, as shown in Figure 6. The weight of the lumped masses and the stiffness of the structural springs from the top to the bottom are assumed to be the following. Weights: 1960, 1176, 1176 (kN); spring stiffness: 19 600, 19 600, 24 500 (kN/m).

The first natural period of the model is about 1·23 s. Internal viscous damping with a factor $h = 0{\cdot}05$ for 1·0 s is assumed for all springs. The controlled forces act laterally at each floor. Half, original and twice El Centro, whose original maximum acceleration is about 3·5 m/s$^2$, excite the model. These excitations are called E*0·5, E*1·0 and E*2·0, respectively.

To compare the performance of the VDD controlled by the proposed law with that of a linear damper, Case VDD and Case LNR are assumed. The assumed parameters are:

*for Case VDD*:

$$\{g_i\} = \{49\,000,\ 49\,000,\ 49\,000\}\ (\mathrm{kN/m})$$

$$\{\eta_{0i}\} = \{4900,\ 4900,\ 4900\}\ (\mathrm{kN\,s/m})$$

$$\{\lambda_i\} = \{0{\cdot}02,\ 0{\cdot}02,\ 0{\cdot}02\}$$

 

*for Case LNR*:

$$\{g_i\} = \{49\,000,\ 49\,000,\ 49\,000\}\ (\mathrm{kN/m})$$

$$\{\eta_{0i}\} = \{2940,\ 2940,\ 2940\}(\mathrm{kN\ s/m})$$

$$\{\lambda_i\} = \{0{\cdot}0,\ 0{\cdot}0,\ 0{\cdot}0\}.$$

The resulting time histories of the VDD's damping coefficient $\eta_2(t)$, the controlled force $u_2(t)$, and the deformation rate $U_2^{\mathrm{T}}y'(t)$ at the second storey for Case VDD and the excitation acceleration E*1·0 are shown in Figure 7, and the controlled force vs. deformation ($u$–$y$) relations at each storey for E*2·0 are shown in Figure 8. Figure 9 shows the maximum controlled forces $u_{\max}$ and the structural spring forces $f_{\max}$ at each storey, comparing Case VDD with Case LNR.

Figure 7(a) shows that $\eta_2(t)$ for E*0·5 mostly remains at a maximum. However, the time history of $\eta_2(t)$ for E*1·0 draws a bumpy line under the influence of the proposed control law. The bumps are deeper for the time history of $\eta_2(t)$ for E*2·0, being greatly influenced by non-linearity. As a result, the controlled force for E*2·0 is smaller than four times that for E*0·5, as shown in Figure 7(b). This relatively small controlled force causes small response reductions, which show large differences in Figure 7(c).

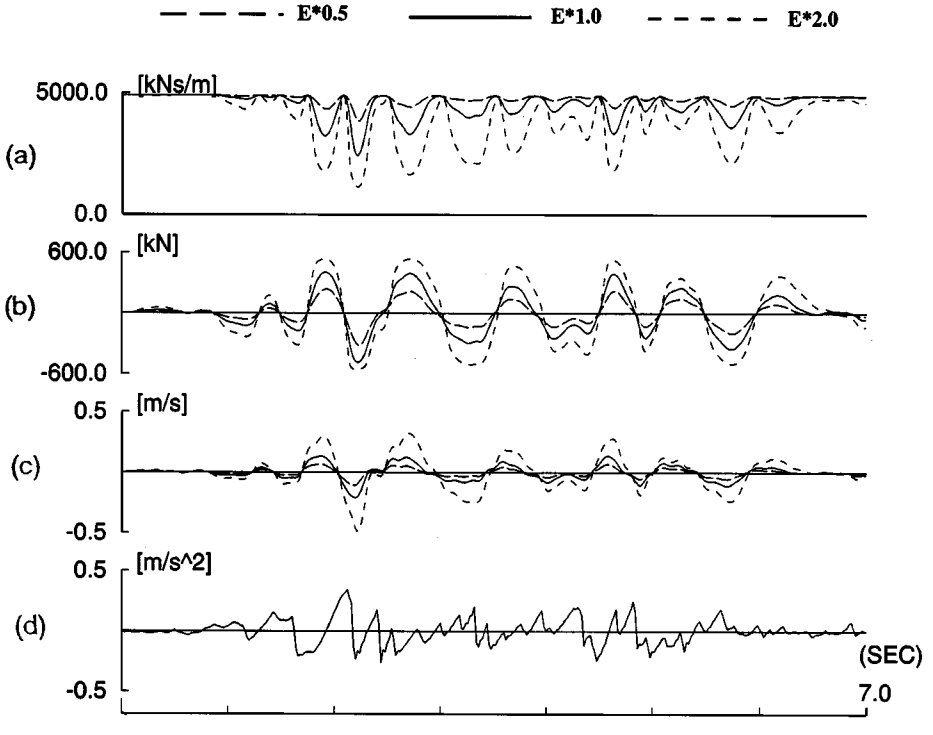


Figure 7. Response time histories at second storey for Case VDD: (a) VDD's damping coefficient; (b) controlled force; (c) deformation rate; (d) input excitation (E*1·0)

 

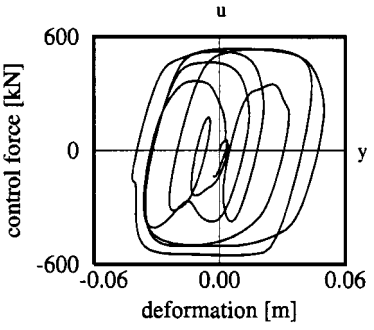


Figure 8. $u$–$y$ relation at second storey for Case VDD for E*2·0

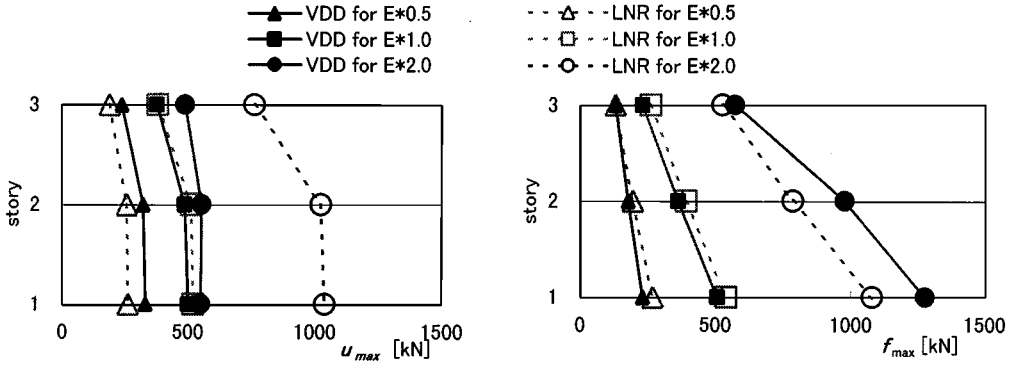


Figure 9. $u_{max}$ and $f_{max}$ at each storey for Case VDD and LNR

Figure 8 shows parallelogram-like hystereses at the second storey for E*2·0. The controlled forces have limit values and dissipate energy by large deformation. That is, the proposed control law can work for the MDOF model as it does for the SDOF model.

As shown in Figure 9, both $u_{max}$ and $f_{max}$ for Case LNR increase in proportion to the excitation levels. However, $u_{max}$ for Case VDD does not increase in proportion to the excitation levels due to the non-linearity of the control law. The $u_{max}$ at each storey for Case VDD for E*2·0 have small increments compared to those for Case VDD for E*1·0 and are almost half of those for Case LNR for E*2·0. The $f_{max}$ for Case VDD for E*2·0 at each storey are about 1·2 times of $f_{max}$ for Case LNR for E*2·0 although $u_{max}$ for the former are half of $u_{max}$ for the latter. This indicates that the VDD controlled by the proposed law works more efficiently in reducing the structural seismic responses than the linear damper.

As described above, the extended control law for plural VDDs attached to the MDOF model can work to efficiently reduce structural seismic responses.

## CONCLUSIONS

(1) A non-linear control law is proposed for a Variable Damping Device (VDD) comprised of a non-linear Maxwell element with an auxiliary stiffness element (ASE). With little external

 

power required to adjust the VDD's damping coefficient, a large amount of the controlled force in the non-linear Maxwell element acts on a structure to reduce its seismic responses.

(2) The control law is introduced by considering a simple non-linear relation between the VDD's damping coefficient and the controlled force. For practical purposes, it is expressed by a non-linear differential equation or in its discretized form, which determines the increment of the VDD's damping coefficient at a certain moment. Because the induction of the control law is simple, the control law for an SDOF model is easily extended to one for an MDOF model.

(3) The controlled force for small deformation can quickly act on a structure like a spring force, while that for large deformation dissipates energy like a damper force. The controlled force vs. deformation relations in the non-linear Maxwell element draws parallelogram-like hysteretic curves. Thus, the controlled force can dissipate a large amount of energy, while restraining its maximum value.

(4) Numerical experiments for SDOF and 3DOF structural models show that the controlled force works more efficiently in reducing the structural seismic responses than a linear damper force.

## REFERENCES


1. P. Mahmoodi, 'Structural dampers', *J. Struct Div.* ASCE **95**, 1661–1672 (1969).
2. T. T. Soon and G. F. Darguch, *Passive Energy Dissipation Systems in Structural Engineering*, Wiley, New York, 1997.
3. J. M. Kelly, R. I. Skinner and A. J. Heine, 'Mechanics of energy absorption in special devices for use in earthquake resistant structures', *Bull. N.Z. Soc. Earthquake Engng.* **5**(3), 63–88 (1972).
4. G. W. Housner, T. T. Soong, and S. D. Masri, 'Second generation of active structural control in civil engineering', *Proc. 1st World Conf. on Struct. Control*, Vol. 1, Panel-3–18, 1994.
5. T. Kobori, 'Structural control for large earthquakes', *Proc. 19th Int. Cong. Theoretical and Applied Mechanics*, Elsevier Amsterdam, 1996, pp. 3–28.
6. G. W. Housner, L. A. Bergman, T. K. Caughey, A. G. Chassiakos, R. O. Claus, S. F. Masri, R. E. Skelton, T. T. Soong, B. F. Spencer and J. T. P. Yao, 'Structural Control: Past, present, and future', *J. Engng. Mech.* ASCE **123**, 897–971 (1997).
7. Q. Feng and M. Shinozuka, 'Use of a variable damper for hybrid control of bridge response under earthquake.', *Proc. U.S. National Workshop on Struct. Contr Res.*, 1990.
8. K. Kawashima, S. Unjoh, and K. Shimizu, 'Experiments on dynamic characteristics of variable damper', *Proc. Japan Nat. Symp. on Struct. Response Control*, 1992, p. 121.
9. M. D. Symans, M. C. Constantinou, D. P. Taylor and K. D. Garnjost, 'Semi-active fluid viscous dampers for seismic response control', *Proc. 1st World Conf. on Struct. Control*, Vol. 3, FA4-3-12, 1994.
10. R. L. Sack and W. N. Patten, 'Seismic hydraulic structural control', *Proc. Int. Workshop on Struct. Control*, 1993, pp. 417–431.
11. E. Polak, G. Meeker, K. Yamada and N. Kurata, 'Evaluation of an active variable-damping structure', *Earthquake Engng. Struct. Dyn.* **23**, 1259–1274 (1994).
12. T. Hatada, and H. A. Smith, 'Development and application of nonlinear controller using variable damping devices', *Proc. American Control Conf.*, 1997, pp. 453–457.
13. N. Kurata, T. Kobori, M. Takahashi, N. Niwa and H. Kurino., 'Shaking table experiment of active variable damping system', *Proc. 1st World Conf. on Struct. Control,* Vol. 2, TP2-108-117, 1994.
14. W. D. Iwan and L. J. Wang, 'New developments in active interaction control', *Proc. of 2nd Int. Workshop on Struct. Control*, 1996, pp. 253–262.
15. H. Kurino, T. Kobori, M. Takahashi, N. Niwa, N. Kurata, Y. Matsunaga and T. Mizuno, 'Development and modeling of variable damping unit for active variable damping system', *Proc. 11th World Conf. of Earthquake Engin*, 1996.
16. T. Kobori, M. Takahashi, T. Nasu, N. Niwa and K. Ogasawara, 'Seismic Response Controlled Structure with Active Variable Stiffness System', *Earthquake Engng Struct. Dyn.* **22**, 925–941 (1993).
17. K. Yamada and T. Kobori, 'Control algorithm for estimating future responses of active variable stiffness structure', *Earthquake Engng Struct. Dyn.* **24**, 1085–1099 (1995).
18. J. Guckenheimer and P. Homes, *Nonlinear Oscillations, Dynamical Systems, and Bifurcations of Vector Fields*, Springer, Berlin, 1983.
19. S. Wiggins, *Introduction to Applied Nonlinear Dynamical Systems and Chaos*, Springer, Berlin, 1990.


 